PROCEEDINGS B

royalsocietypublishing.org/journal/rspb

Research

Cite this article: Chen X, Fu F. 2019 Imperfect vaccine and hysteresis. *Proc. R. Soc. B* **286**: 20182406.
http://dx.doi.org/10.1098/rspb.2018.2406

Received: 25 October 2018
Accepted: 3 December 2018

Subject Category:
Evolution

Subject Areas:
health and disease and epidemiology, evolution

Keywords:
vaccine efficacy, evolutionary dynamics, social imitation, hysteresis loop

Author for correspondence:
Feng Fu
e-mail: fufeng@gmail.com

Electronic supplementary material is available online at https://dx.doi.org/10.6084/m9.figshare.c.4334363.

THE ROYAL SOCIETY PUBLISHING

Imperfect vaccine and hysteresis

Xingru Chen[1] and Feng Fu[1,2]

[1]Department of Mathematics, Dartmouth College, Hanover, NH 03755, USA
[2]Department of Biomedical Data Science, Geisel School of Medicine at Dartmouth, Lebanon, NH 03756, USA

FF, 0000-0001-8252-1990

Addressing vaccine compliance problems is of particular relevance and significance to public health. Despite resurgence of vaccine-preventable diseases and public awareness of vaccine importance, why is it so challenging to boost population vaccination coverage to desired levels especially in the wake of declining vaccine uptake? To understand this puzzling phenomenon, here we study how social imitation dynamics of vaccination can be impacted by the presence of imperfect vaccine, which only confers partial protection against the disease. Besides weighing the perceived cost of vaccination with the risk of infection, the effectiveness of vaccination is also an important factor driving vaccination decisions. We discover that there can exist multiple stable vaccination equilibria if vaccine efficacy is below a certain threshold. Furthermore, our bifurcation analysis reveals the occurrence of *hysteresis loops* of vaccination rate with respect to changes in the perceived vaccination cost as well as in the vaccination effectiveness. Moreover, we find that hysteresis is more likely to arise in spatial populations than in well-mixed populations, even for parameter choices that do not allow for bifurcation in the latter. Our work shows that hysteresis can appear as an unprecedented roadblock for the recovery of vaccination uptake, thereby helping explain the persistence of vaccine compliance problem.

1. Introduction

Mass vaccination is one of the most cost-effective means to prevention and control of infectious diseases [1–3]. Thanks to the advent of modern vaccines, millions of lives have been saved [4]. Despite these known facts about the importance of vaccine, it remains a huge challenge to achieve desirable vaccination coverage in order for herd immunity to be in effect [5–7]. Moreover, the long-standing dilemma of voluntary vaccination is exacerbated by spreading concerns about vaccine safety and efficacy [8–10]. In recent years, considerable attention has been paid to improving our understanding of the role of social factors in epidemiology [11–17].

In particular, the use of behaviour–disease interaction models has become an important approach to study how vaccine compliance can be influenced by a wide range of factors [18–24], ranging from vaccine scares [25] to disease awareness [26]. Prior work shows that a misalignment between individual interest and the population interest can cause suboptimal vaccination coverage [27–30], thereby leading to a tragedy of the commons in vaccination uptake [31].

Moreover, vaccine may be imperfect in the sense that (i) there can exist unwanted, adverse side effects of various degrees, albeit being minor most of the time, causing exaggerated perceived risk or cost of vaccination [8,9,32], and (ii) vaccination only can confer partial protection against the disease [33–35], also known as primary and secondary vaccine failures [36–38]. Indeed, the presence of imperfect vaccine can diminish public confidence in vaccine and thus erode an individual's intention to vaccinate [39–44]. Although the efficacy and cost-effectiveness of vaccination has been a topic of extensive investigation [45–52], the complications of imperfect vaccine on uptake behaviour have not been fully understood yet [39,40,42,43,53,54].

Notably, in the aftermath of a sharp decline in vaccination coverage triggered by concerns regarding vaccine safety and efficacy, the recovery of vaccination rate from nadir to levels needed to attain herd immunity has been remarkably

slow [39,40,55–59]. For example, it took almost 15 years for the recovery in the uptake of whole-cell pertussis vaccine from rock bottom 30% in 1978 to 91% in 1992 in England and Wales [55]. More recently, even though resurgent measles outbreaks impose huge risks for those unvaccinated, and even in some regions like France it has become an endemic disease [57,58], the coverage of measles vaccination has only gradually climbed up, but still remains insufficient, more than a decade after the infamous MMR vaccination and autism controversy [40,59]. It seems that the recovery of vaccination rate depends not just on the extent of mitigating perceived cost of vaccination and improving vaccine efficacy, but also on the past vaccination trajectory, hence possibly marring a rapid increase.

To shed light on this puzzling phenomenon, here we explicitly take into account the role of both vaccination cost and effectiveness in individual vaccination decisions. Surprisingly, we discover that hysteresis loops can arise in social imitation dynamics of vaccination behaviour. Hysteresis effect makes the vaccination coverage sensitive to changes in factors that drive vaccination decisions such as the cost and effectiveness and also hinders recovery of vaccine uptake.

2. Results and discussion

To quantify the risk of infection during an epidemic outbreak, we first consider an epidemiological process in well-mixed populations, using the susceptible–infected–recovered with preemptive vaccination (SIR-V) model. The infection risk, w_0, for an unvaccinated individual is $1-\exp[-R_0R(\infty)]$, and the infection risk, w_1, for a vaccinated individual is $1-\exp[-(1-\varepsilon)R_0R(\infty)]$. Here, R_0 is the basic reproductive ratio of the disease, ε denotes the effectiveness of vaccination and $R(\infty)$ is the final epidemic size, which is implicitly dependent on the population vaccination level, x. Assume the relative cost of vaccination to infection is $c \in (0, 1)$. Up to a positive constant factor, the expected payoff for an unvaccinated individual is $f_0(x) = -w_0(x)$ and for a vaccinated individual $f_1(x) = -c[1 - w_1(x)] - (1 + c)w_1(x)$. Denote their payoff difference by $F(x) = f_1(x) - f_0(x)$. The social imitation dynamics of vaccination behaviour can be described by the replicator equation [60–62],

$$\frac{\mathrm{d}x}{\mathrm{d}t} = x(1-x)F(x), \tag{2.1}$$

which governs the time evolution of the fraction of vaccinated individuals, x, over epidemic seasons.

The possible interior equilibrium x^* can be found by solving the fixed points of $F(x) = 0$. As shown in figure 1, there can exist multiple interior equilibria of vaccination level, x^*, under certain parameter combinations of c and ε. To gain further insights into understanding such bistability of equilibrium vaccination level x^*, we find the following implicit equations that describe the dependence of x^* on c and ε intermediately through the final epidemic size $R(\infty)$:

$$c = \exp[-(1-\varepsilon)R_0R(\infty)] - \exp[-R_0R(\infty)] \tag{2.2}$$

and

$$x^* = \frac{R(\infty) + \exp[-R_0R(\infty)] - 1}{\exp[-R_0R(\infty)] - \exp[-(1-\varepsilon)R_0R(\infty)]}. \tag{2.3}$$

These closed-form formulae allow us to perform a thorough bifurcation analysis based on the bistability condition

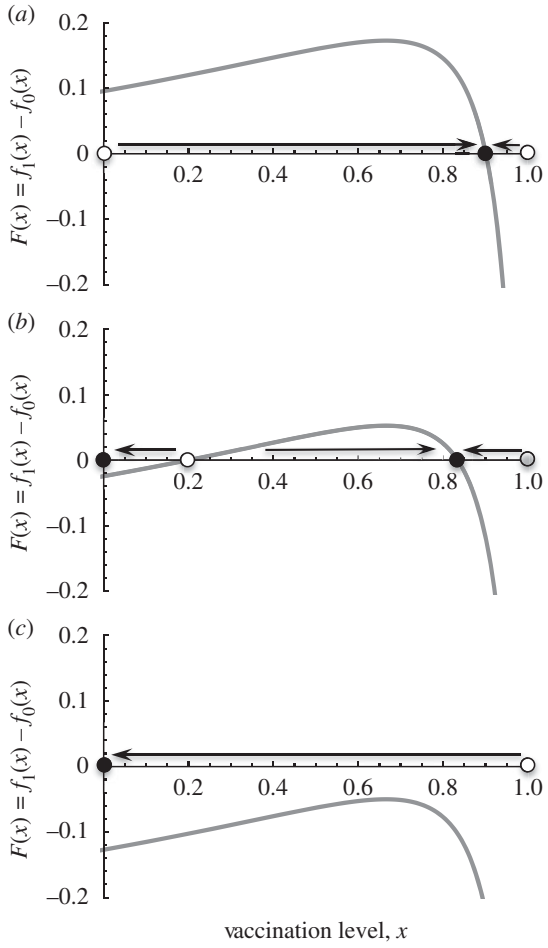

Figure 1. Bistability in vaccination dynamics. There can exist multiple stable equilibrium vaccination levels if vaccine is imperfect that cannot provide sufficient protection against contracting the disease. Shown are the expected payoff differences between vaccinated and unvaccinated individuals as a function of the vaccination level x for increasing relative costs of vaccination $c =$ (*a*) 0.3, (*b*) 0.42 and (*c*) 0.52, in an infinite, well-mixed population. Solid circles indicate stable equilibria, and empty circles unstable equilibria. Parameters: vaccine effectiveness, $\varepsilon = 0.75$, and basic reproductive ratio, $R_0 = 3.5$.

(figure 2). As detailed in the electronic supplementary material, we can show that for bistability to occur, R_0 and the effectiveness of vaccination ε must satisfy the inequality

$$-\frac{\ln(1-\varepsilon)}{\varepsilon[1-(1-\varepsilon)^{1/\varepsilon}]} < R_0 < \frac{1}{1-\varepsilon}. \tag{2.4}$$

Of particular interest is the existence of a minimum lower bound for R_0. We find R_0 must exceed $e/(e-1) \approx 1.58$ in order for bifurcation to occur in well-mixed populations, where e is the base of natural logarithm (cf. figure 2*b*,*c* and *d*,*e*). The social optimum of vaccination level is given by the herd immunity threshold $x_h = (R_0 - 1)/(\varepsilon R_0)$. The constraint of $x_h \leq 1$ leads to the upper bound of $R_0 \leq 1/(1-\varepsilon)$.

Furthermore, for given ε satisfying the above inequality (2.4), we can derive the exact range of $c \in (c_l, c_h)$ that allows for bistability:

$$c_l = \exp[-(1-\varepsilon)R_0R(\infty)_m] - \exp[-R_0R(\infty)_m] \tag{2.5}$$

and

$$c_h = (1-\varepsilon)^{(1-\varepsilon)/\varepsilon} - (1-\varepsilon)^{1/\varepsilon}, \tag{2.6}$$

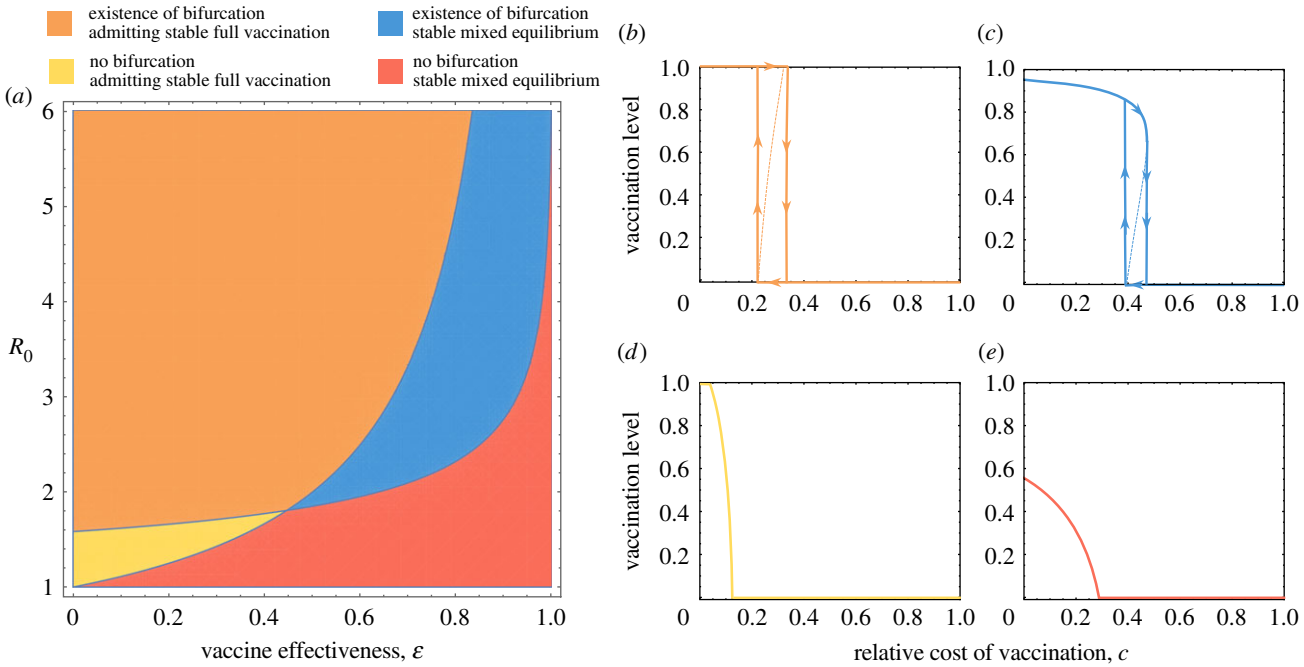

Figure 2. Bifurcation conditions and hysteresis loops of population vaccination equilibrium in well-mixed populations. (*a*) The combination of parameters ε and R_0 required for the occurrence of bifurcation in equilibrium vaccination level, that is, $-\ln(1-\varepsilon)/(\varepsilon(1-(1-\varepsilon)^{1/\varepsilon})) < R_0 < 1/(1-\varepsilon)$ (see main text for details). These two bounds of R_0 expressed in closed forms of ε divide the parameter space (ε, R_0) into four regions that result in different vaccination dynamics, as shown in (*b*–*e*). For $R_0 > 1/(1-\varepsilon)$ (namely, the social optimum vaccination level $(R_0-1)/(\varepsilon R_0) > 1$, which is impossible), bifurcation can still occur, but full vaccination can emerge as a stable equilibrium, revealing a paradox in which 'the number is traded for efficiency'. (*b*,*c*) How the hysteresis loop of the equilibrium vaccination level can arise: for the descending path of the hysteresis loop, the vaccination level decreases with c and plunges into zero if c further exceeds a threshold value c_h. For the ascending path, the equilibrium vaccination level remains at zero even if c has dropped below the threshold value c_h, but will be able to recover to a high level if $c < c_l$. The dashed lines in (*b*,*c*) indicate the unstable interior equilibrium separating the basins of attraction for the other two stable equilibria located on the hysteresis loop. (*d*,*e*) No bifurcation is admissible for $R_0 < -\ln(1-\varepsilon)/(\varepsilon(1-(1-\varepsilon)^{1/\varepsilon}))$ and there only exists one stable equilibrium vaccination level. Parameters: (*b*) $R_0 = 3.5$, $\varepsilon = 0.6$, (*c*) $R_0 = 3.5$, $\varepsilon = 0.75$, (*d*) $R_0 = 1.5$, $\varepsilon = 0.3$, (*e*) $R_0 = 1.5$, $\varepsilon = 0.6$. (Online version in colour.)

where $R(\infty)_m$ is the largest possible epidemic size with zero vaccination coverage, given by $R(\infty)_m + \exp[-R_0 R(\infty)_m] - 1 = 0$.

Taken together, the existence of bistability directs us to perform a further bifurcation analysis of vaccination equilibrium with respect to changes in the relative cost of vaccination, c, and the effectiveness of vaccination, ε. As plotted in figure 2*a*, the conditions of equation (2.4) divide the parameter space (ε, R_0) into four regions, in which different vaccination dynamics can happen accordingly (figure 2*b*–*e*). Interestingly, in the region $R_0 > 1/(1-\varepsilon)$, despite substantially low effectiveness of vaccination, bifurcation still can occur, and full vaccination appears as a unique stable equilibrium for small relative costs of vaccination c (figure 2*b*). This seemingly counterintuitive result can be understood as resulting from 'the number is traded for efficiency': as the risk of infection for unvaccinated is substantially higher than that for vaccinated even in the presence of comprised vaccination effectiveness, choosing to vaccinate still leads to a better prospect of payoff than not to, thereby causing the population to be fully vaccinated in equilibrium. It is worth noting that, in spite of such elevated vaccine take-up, the effective vaccination coverage actually reduces and thus results in larger epidemic sizes (see electronic supplementary material, figure S4b).

When both conditions of equation (2.4) are met, the equilibrium vaccination level at $c = 0$ coincides with the social optimum $x_h = (R_0-1)/(\varepsilon R_0)$, but it becomes short of levels needed to maintain herd immunity as c increases (figure 2*c*). Bifurcation occurs in the range of relative cost of vaccination (c_l, c_h), in which both zero coverage and the larger interior equilibrium, separated by another smaller unstable interior equilibrium, are stable. For $c \geq c_h$, zero vaccination coverage is the only stable equilibrium. No bifurcation is admissible for $R_0 < -\ln(1-\varepsilon)/[\varepsilon(1-(1-\varepsilon)^{1/\varepsilon})]$, as demonstrated in figure 2*d*,*e*.

As revealed by our bifurcation analysis, hysteresis loops of vaccination rate can arise with respect to changes in the perceived cost of vaccination c (figure 2*c*). In the presence of imperfect vaccine, if the public perception exaggerates the real cost of vaccination, which should be quite small otherwise, the vaccine uptake can plunge from high levels into zero if c exceeds c_h, corresponding to the descending path of the hysteresis loop. In stark contrast, the recovery of vaccination rate takes a different route, namely, the ascending path of the hysteresis loop, and is inhibited until the perceived cost of vaccination c is mitigated less than c_l. Thus, the occurrence of hysteresis debilitates public health effort in promoting vaccination, as hysteresis effect simply hinders the recovery of vaccine uptake. This is an important insight arising from our present study.

Moreover, we validate our theoretical analysis of hysteresis using agent-based simulations (figure 3). For practical reasons, we consider imitation dynamics of vaccination in a finite, well-mixed population and obtain the hysteresis loops with respect to changes in c and ε by Monte Carlo simulations (see Methods and Model section). Although our analytical results are derived for infinitely large populations, they are in good agreement with stochastic simulation results, with discrepancies owing to the finite-size effects. Similar to the hysteresis loop with respect to c for fixed ε (figure 3*a*, and also figure 2*c*), the bifurcation and hysteresis loop can

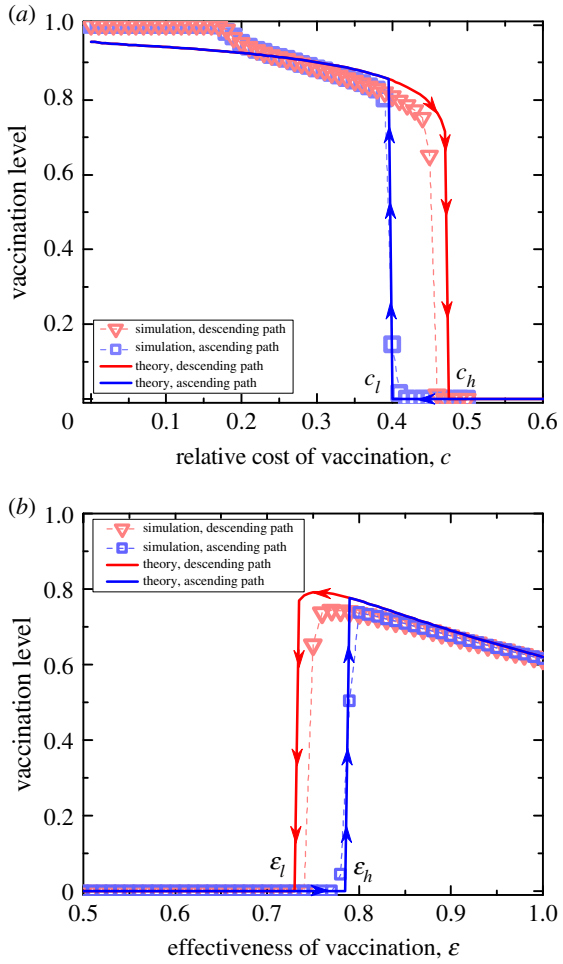

Figure 3. Hysteresis in well-mixed populations. Shown are the occurrence of hysteresis loop of equilibrium vaccination levels with respect to changes in (*a*) relative cost of vaccination, c, and (*b*) vaccine effectiveness, ε. Our theoretical predictions are in good agreement with agent-based simulation results. Parameters: population size $N = 1000$, number of infection seeds $I_0 = 10$, transmission rate $\beta N = 0.35$, recovery rate $\gamma = 0.1$, (*a*) vaccine effectiveness $\varepsilon = 0.75$, (*b*) relative cost of vaccination $c = 0.45$. Simulation results are averaged over 50 independent runs. (Online version in colour.)

arise as well when varying the effectiveness of vaccination ε. We note that for the fixed relative cost of vaccination $c = 0.1$, the equilibrium vaccination level first increases as the effectiveness of vaccination ε reduces from 100% until reaching a plateau of full vaccination, but it plummets into zero if ε is less than ε_l, corresponding to the descending path of the hysteresis loop (figure 3*b*). Moreover, in the ascending path, albeit with increasing ε above ε_l, the zero vaccination level remains stable until ε increases beyond another threshold ε_h (also see electronic supplementary material, figure S4a).

These two critical values of ε illuminate the complications of imperfect vaccine on vaccination compliance. No individuals would choose to vaccinate if the vaccine efficacy has slipped below the critical threshold ε_l. Owing to the presence of hysteresis loop, the vaccination coverage cannot be immediately boosted with little improvement in ε, unless $\varepsilon > \varepsilon_h$. Furthermore, overshooting of vaccination behaviour can occur as a consequence of slightly comprised vaccination effectiveness, yet such increase in vaccination coverage cannot adequately offset the loss in the efficacy of herd immunity. As a result, the final epidemic size $R(\infty)$ is always monotonically increasing with decreasing ε (see electronic supplementary material, figure S4b).

Aside from well-mixed populations, we now turn our attention to the study of vaccination dynamics in spatial populations. Individuals are situated on a square lattice with von Neumann neighbourhood. Such population structure restricts whom individuals can imitate, or be infected by, to just their immediate neighbours. Individuals' vaccination decisions and health outcomes determine their payoffs. They can revisit their vaccination choices by imitating more successful strategies among their immediate neighbours. As plotted in figure 4*a*,*b* ($R_0 = 1.5$), we show that hysteresis behaviour of population vaccination equilibrium is more likely to arise in spatially structured populations than in well-mixed populations, even for the parameter choices of R_0 and ε that do not allow for bifurcation and hysteresis in the latter. Although spatial population structure can promote vaccination for small c and high ε, the vaccination equilibrium is sensitive to the increase in the perceived cost of vaccination and the reduction in the vaccination effectiveness (cf. figure 4*a*,*b* and figure 3). Figure 4*c*,*d* are spatial snapshots of the population states taken, respectively, at the descending and ascending path of the hysteresis loop in figure 4*a*. One can see that, in comparison with figure 4*d*, the vaccination level in figure 4*c* is significantly higher along with much larger average cluster size of vaccinators, thus resulting in better population health outcomes. We also study vaccination dynamics in random network populations (reported in the electronic supplementary material), and we observe similar results as shown in figure 4.

We also extend our basic model to investigate different scenarios of vaccine failure, namely, waning efficacy of protection from vaccination received at younger ages (so-called secondary vaccine failure; see Methods and model, and the electronic supplementary material). As in previous studies [1,63], we consider an age-structured population with five age classes [0 4], [5 9], [10 14], [15 19] and [20 75] (figure 5). The rates of contact within and between each age class are mediated by the mixing matrix Φ, thus posing heterogeneous degrees of vulnerability to disease outbreaks. Waning protection from prior vaccination in older age groups can substantially comprise the disease control effort by mass vaccination (cf. figure 5*a*,*b*). Figure 5*c*,*d* demonstrate that bifurcation and hysteresis of equilibrium vaccination levels can also arise in age-structured populations as a result of secondary vaccine failure.

More recently, there has been growing interest in studying behaviour–disease interactions, or more generally, the coupled human–environment systems [64], from the lens of dynamical systems. The occurrence of hysteresis is traditionally associated with magnetic properties of materials [65], and also has been found in biological and socio-economical systems [66,67]. In this paper, we show that bifurcation and hysteresis can occur in the important context of public health and vaccination behaviour in particular.

Our work demonstrates that vaccination dynamics can exhibit hysteresis effect (with respect to the changes in the perceived cost of vaccination c) if the vaccine efficacy is lower than a certain threshold ε_c, as given in the inequality (2.4). Depending on the specific immunological mechanisms of vaccination, vaccine efficacy varies from highly effective such as measles vaccine to marginally effective like flu vaccine. To be concrete, for $R_0 = 10$ comparable to measles, we obtain $\varepsilon_c \approx 99.996\%$, which is higher than the current measles vaccine efficacy 95% [42,49,57–59]. As suggested by our analysis, hysteresis

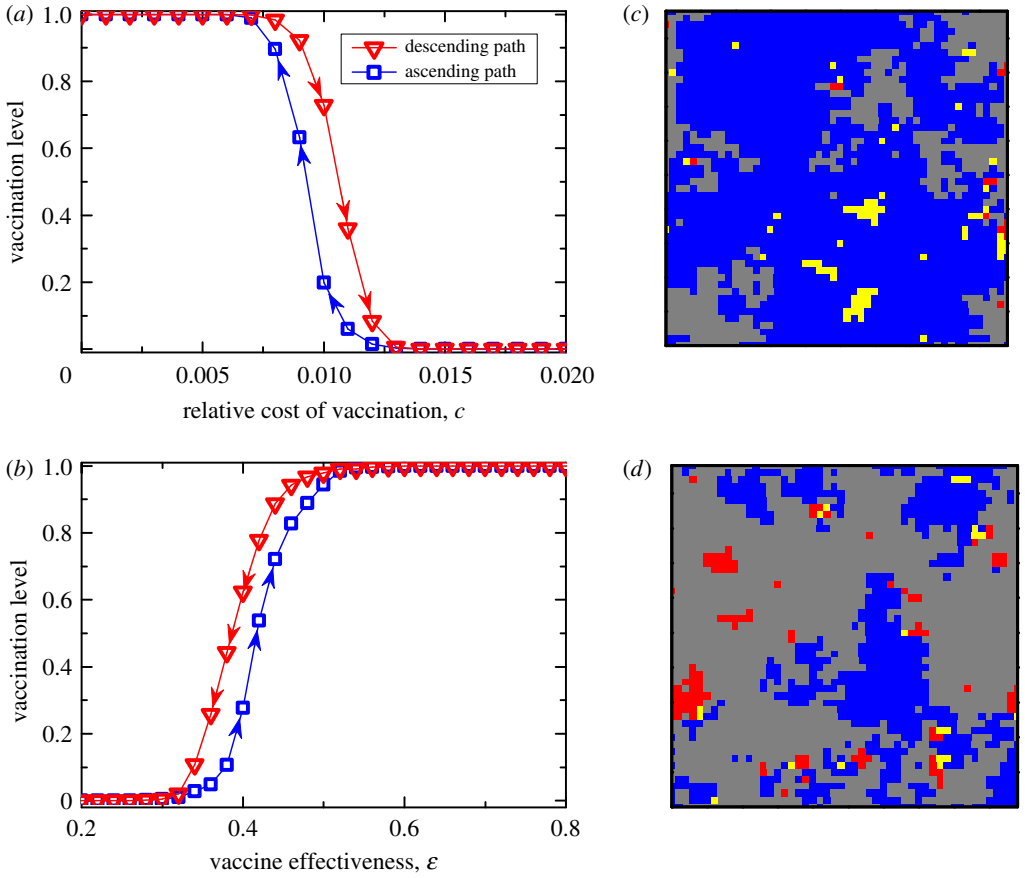

Figure 4. Hysteresis in lattice populations. Hysteresis behaviour of population vaccination equilibrium is more likely to arise in spatial populations than in well-mixed populations, even for the parameter choices of R_0 and ε that do not allow bifurcation and hysteresis in the latter. Shown are the occurrence of hysteresis loop with respect to changes in (*a*) relative cost of vaccination, c, and (*b*) vaccine effectiveness, ε. (*c*,*d*) Snapshots of spatial population states, respectively, in the descending and ascending path of the hysteresis loop in (*a*) for $c = 0.01$ and $\varepsilon = 0.4$. Blue denotes individuals who were vaccinated and remained healthy during the season, yellow denotes individuals who were vaccinated but still got infected, grey denotes individuals who were unvaccinated yet remained healthy, and red denotes individuals who were unvaccinated and got infected. Parameters: square lattice 50×50 with von Neumann neighbourhood, number of infection seeds $I_0 = 30$, transmission rate $\beta = 0.0375$, recovery rate $\gamma = 0.1$, (*a*) $\varepsilon = 0.4$, (*b*) $c = 0.01$. Simulation results are averaged over 100 independent runs. (Online version in colour.)

effect can act as a roadblock for the recovery of measles vaccination coverage, despite resurgent measles outbreaks that impose huge infection risks for these intentionally unvaccinated. Our results also suggest that the effectiveness of vaccination has a substantial impact on vaccine uptake decisions, for example, whether to get flu shots (see figure 4*b*, with model parameters comparable to the case of flu vaccination). In order for the population to achieve high levels of flu vaccination, the efficacy of flu vaccine has to reach above 50%. However, such improvement of the flu vaccine efficacy may turn out difficult due to the fast pathogen mutation and adaptation [68].

The perceived cost or effectiveness of vaccination may be determined by a concurrent dynamic of social contagion that governs the changes in public perception of vaccination risk or vaccine beliefs [69]. In the electronic supplementary material, we show that incorporating co-evolving vaccine attitudes into vaccination dynamics can strengthen the hysteresis effect, further hindering the recovery of vaccine uptake.

In summary, we study how social imitation dynamics of vaccination is affected by the presence of imperfect vaccine, and discover that hysteresis effect can arise under certain conditions. We perform thorough bifurcation analysis across the model parameter space, and moreover, provide exact, closed-form conditions for bifurcation and hysteresis in well-mixed populations. Extending the analysis to spatial populations, we find similar hysteresis phenomenon, which is, in fact, more likely to occur than in well-mixed populations. Our work offers a novel mechanistic explanation for the slow recovery of vaccine uptake, as hysteresis effect can appear as an unprecedented roadblock to efforts for boosting vaccination rates. Nevertheless, as vaccination dilemma is just one example of real-world human cooperation problems, well-studied mechanisms for promoting altruistic behaviour can be leveraged to overcome such hysteresis effect and thus improve vaccine compliance [16,17,70].

3. Methods and model

(a) Basic model

We model the vaccination dynamics as a two-stage game. At stage one, individuals make vaccination decisions that will determine their risk of infection during the epidemic season. Let us assume vaccination takes a relative cost $0 < c < 1$ to infection. At stage two, health outcomes determine individuals' final payoffs. The risk of infection can be calculated using an epidemiological process as follows.

To account for the effectiveness of vaccination, we introduce the parameter $\varepsilon \in [0, 1]$ in the SIR-V model for

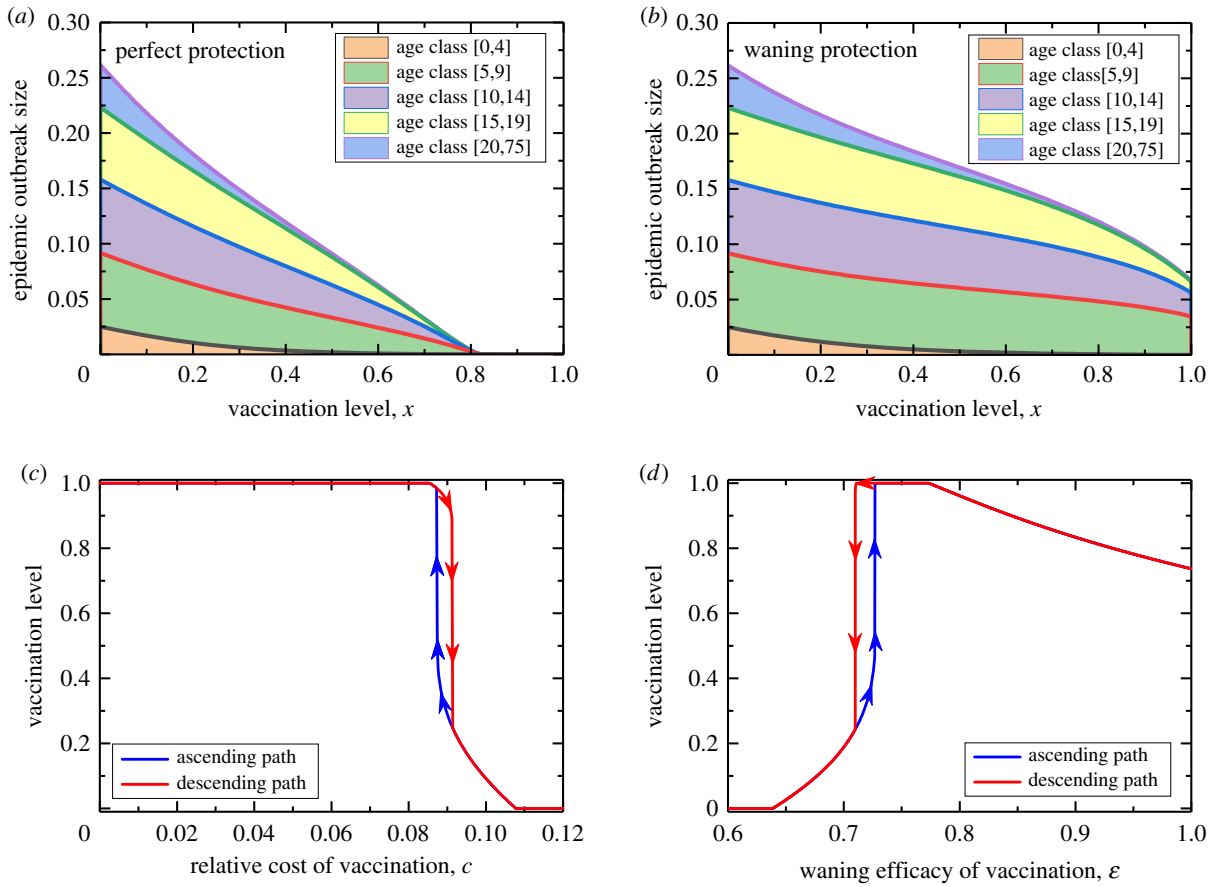

Figure 5. Hysteresis in age-structured populations with waning vaccine protection. (*a*,*b*) The stacked area plot of the epidemic outbreak size in each age class as a function of the vaccination level, x, respectively, with (*a*) perfect vaccine protection and (*b*) waning protection with the vaccine efficacy reduced for age groups 5 and above. (*c*,*d*) The occurrence of hysteresis loops of equilibrium vaccination levels with respect to changes in (*c*) the cost of vaccination, c, and (*d*) the waning efficacy of vaccination, ε. Parameters: (*a*–*d*) $\hat{\alpha} = \left[\frac{1}{15}, \frac{1}{15}, \frac{1}{15}, \frac{1}{15}, \frac{11}{15}\right]$, $\Phi = \{\phi_{ij}\}$ with $\phi_{ij} = 0.05$ for $i \neq j$ and $\phi_{ii} = 0.8$, $\hat{\beta} = [0.3, 5, 4, 3, 0.06]$, $\hat{\gamma} = [0.015, 0.05, 0.05, 0.05, 0.05]$, (*a*) $\hat{\varepsilon} = [1, 1, 1, 1, 1]$, (*b*) and (*c*) $\hat{\varepsilon} = [1, 0.75, 0.75, 0.75, 0.75]$, (*d*) $c = 0.08$, $\hat{\varepsilon} = [1, \varepsilon, \varepsilon, \varepsilon, \varepsilon]$. (Online version in colour.)

disease spreading:

$$\left.\begin{aligned} \frac{dS}{dt} &= -\beta SI, \\ \frac{dI}{dt} &= \beta SI + (1-\varepsilon)\beta VI - \gamma I, \\ \frac{dV}{dt} &= -(1-\varepsilon)\beta VI \\ \text{and} \quad \frac{dR}{dt} &= \gamma I. \end{aligned}\right\} \tag{3.1}$$

Here, the transmission rate of the disease to an unvaccinated individual is β, compared with $(1-\varepsilon)\beta$ for a vaccinated individual. Thus the parameter ε quantifies the effectiveness of vaccination for protecting against the disease. For perfect vaccines, $\varepsilon = 1$, vaccinated individuals have zero risk of infection, as analysed in previous studies [20]. For imperfect vaccines, $0 < \varepsilon < 1$, vaccinated individuals still face the risk of getting infected but with a reduced likelihood than unvaccinated individuals. Unlike previous models [10], where vaccination provides full protection with certain probability or otherwise completely fails as if unvaccinated, in this study we assume vaccination provides partial protection for every vaccinated individual. This scenario is also known as the primary vaccine failure. In our model extensions (see details in the electronic supplementary material), we also consider secondary vaccine failure in which the waning of protection occurs over time elapsed since vaccination [36–38].

Individuals can revisit their vaccination decision in between epidemic seasons. Simple social learning processes can be represented by imitation dynamics under peer influence, through which process individuals try to learn vaccination strategies that are more successful (i.e. higher payoffs). Following common practice in prior work [14], we use the replicator dynamics to account for such social imitation of vaccination dynamics. Let x denote the fraction of vaccinated individuals in the population. The evolutionary dynamics of vaccination behaviour can be described by the following differential equation (the appropriate time scales will be seasons):

$$\dot{x} = x(1-x)F(x). \tag{3.2}$$

Here, $F(x)$ denotes the payoff difference between a vaccinated and unvaccinated individual. Investigation of possible fixed points of $F(x)$ tells us about the interior equilibrium (mixed) of vaccination level x^* and their evolutionarily stability.

(b) Simulation methods

In our stochastic agent-based simulations, we simulate the epidemic spreading process that determines the health outcomes of individuals using the Gillespie algorithm [71]. In the stage of updating vaccination strategy, a focal individual

i randomly picks up one neighbour individual j, and adopts j's vaccination strategy s_j with the probability given by

$$W_{s_i \leftarrow s_j} = \frac{\pi_j - \pi_i}{\Delta_{\max}}, \tag{3.3}$$

where π_i and π_j are the payoffs of individual i and j, and the denominator $\Delta_{\max}$ is a normalization factor such that the absolute value of $W_{s_i \leftarrow s_j}$ is within one. Instead of the expected payoffs used in equation (3.2), we use the actual payoffs, that is,

$$\pi_i = \begin{cases} -c, & \text{vaccinated, and remained healthy} \\ -c-1, & \text{vaccinated, but got infected} \\ -1, & \text{unvaccinated, and got infected} \\ 0, & \text{unvaccinated, and remained healthy.} \end{cases}$$

Here, we choose $\Delta_{\max}$ to be $1 + c$. This updating rule has been called as the 'replicator dynamic' [72]. In the limit of infinitely large populations, the stochastic dynamics are shown to converge to the deterministic replicator equation, up to a constant factor [73].

We perform similar stochastic simulations in lattice populations with the von Neumann neighbourhood [74,75]. In this case, individuals can only be infected by, or imitate from, immediate neighbours.

To determine equilibrium vaccination levels, we run each simulation with specified initial conditions first for 3000 steps and then average the vaccination level over steps from 3000 to 4000. We further average this over 50–100 independent runs. Our results are robust with respect to changes in simulation steps. To obtain the hysteresis loop by simulations, we start the simulation with increasing costs of vaccination c_i specified by the sequence $0 < c_1 < c_2 < c_3 < \cdots < 1$ (with decreasing effectiveness of vaccination $1 > \varepsilon_1 > \varepsilon_2 > \varepsilon_3 > \cdots > 0$, respectively). For each parameter choice, we obtain the equilibrium vaccination as mentioned above and use this equilibrium at c_i (ε_i) as the initial condition for the next run with the parameter value c_{i+1} (ε_{i+1}), and subsequently obtain the equilibrium value under this new parameter value, and so on. In this way, we obtain the descending path of the hysteresis loop. For the ascending path, we just do the same but reverse the sequence order in varying the parameters. By simulating different population sizes, we confirm that no pronounced effect is observed in the simulation results, including the width of the hysteresis loop (i.e. the parameter range over which the hysteresis occurs), due to the specific lattice size used in figure 4.

If the population enters absorbing states due to finite population size effects, we need to perturb the system into a mixed population state as the prescribed initial input for the subsequent simulation runs. Specifically, we use the frequency of 95% vaccinated as the initial condition for the next parameter run if the population enters full vaccination in the previous parameter run, and similarly we use 5% vaccinated as the initial condition if the population enters zero vaccination in the previous parameter run. We confirm that small variations with respect to choices of these initial conditions do not qualitatively change our simulation results.

(c) Model extensions

To study secondary vaccine failure, we extend the basic model with an age structure that depicts different mixing contacts and therefore heterogeneous risks of infection among n age classes. For simplicity, we suppose that a fraction x of each age cohort is vaccinated, essentially at birth. This assumption is appropriate for studying childhood diseases, as most types of childhood immunization are scheduled more or less within 12 months of birth. As detailed in the electronic supplementary material, the age-structured epidemiological model is similar to equation (3.1), except for using age-specific parameters, which are given by the vector of transmission rates $\hat{\beta} = [\beta_1, \beta_2, \ldots, \beta_n]$, recovery rates $\hat{\gamma} = [\gamma_1, \gamma_2, \ldots, \gamma_n]$, and vaccine efficacies $\hat{\varepsilon} = [\varepsilon_1, \varepsilon_2, \ldots, \varepsilon_n]$, for each age class $a = 1, 2, \ldots, n$, respectively. The parameter ε_a quantifies the degree of waning of vaccine protection for individuals in age class a who had received vaccination shortly after birth. Denote the population proportion of each age class by $\hat{\alpha} = [\alpha_1, \alpha_2, \ldots, \alpha_n]$. The force of infection for the age class a is $\beta_a(\sum_{j=1}^{n} \phi_{aj} I_j)$, where the elements ϕ_{aj} of the mixing matrix Φ mediate the rates of contact between and within age classes. The overall risks of infection for vaccinated versus unvaccinated across age classes determine vaccine uptake decisions.

Ethics. Ethical assessment is not required prior to conducting the research reported in this paper, as the present study does not have experiments on human subjects and animals, and does not contain any sensitive and private information.

Data accessibility. All pertinent analysis has been included in the main text and in the electronic supplementary material.

Authors' contributions. X.C. and F.F. conceived the model, performed analyses and wrote the manuscript.

Competing interests. We declare we have no competing interests.

Funding. We are grateful for support from the G. Norman Albree Trust Fund, Dartmouth Faculty Startup Fund, Walter & Constance Burke Research Initiation Award and NIH Roybal Center Pilot Grant.

Acknowledgements. We thank three anonymous referees for their constructive and insightful comments.

References

1. Anderson RM, May RM, Anderson B. 1992 *Infectious diseases of humans: dynamics and control*, vol. 28. Chichester, UK: Wiley Online Library.
2. Hethcote HW. 2000 The mathematics of infectious diseases. *SIAM Rev.* **42**, 599–653. (doi:10.1137/S0036144500371907)
3. Levin BR, Lipsitch M, Bonhoeffer S. 1999 Population biology, evolution, and infectious disease: convergence and synthesis. *Science* **283**, 806–809. (doi:10.1126/science.283.5403.806)
4. Bärnighausen T, Bloom DE, Cafiero-Fonseca ET, O'Brien JC. 2014 Valuing vaccination. *Proc. Natl Acad. Sci. USA* **111**, 12 313–12 319. (doi:10.1073/pnas.1400475111)
5. Bloom BR, Marcuse E, Mnookin S. 2014 Addressing vaccine hesitancy. *Science* **344**, 339. (doi:10.1126/science.1254834)
6. Fine P, Eames K, Heymann DL. 2011 'Herd immunity': a rough guide. *Clin. Infect. Dis.* **52**, 911–916. (doi:10.1093/cid/cir007)
7. Wadman M, You J. 2017 The vaccine wars. *Science* **356**, 364–365. (doi:10.1126/science.356.6336.364)
8. Chen RT. 1999 Vaccine risks: real, perceived and unknown. *Vaccine* **17**, S41–S46. (doi:10.1016/S0264-410X(99)00292-3)
9. Amanna I, Slifka MK. 2005 Public fear of vaccination: separating fact from fiction. *Viral Immunol.* **18**, 307–315. (doi:10.1089/vim.2005.18.307)

10. Wu B, Fu F, Wang L. 2011 Imperfect vaccine aggravates the long-standing dilemma of voluntary vaccination. *PloS ONE* **6**, e20577. (doi:10.1371/journal.pone.0020577)
11. Bauch CT, Galvani AP. 2013 Social factors in epidemiology. *Science* **342**, 47–49. (doi:10.1126/science.1244492)
12. Wang Z, Bauch CT, Bhattacharyya S, d'Onofrio A, Manfredi P, Perc M, Perra N, Salathé M, Zhao D. 2016 Statistical physics of vaccination. *Phys. Rep.* **664**, 1–113. (doi:10.1016/j.physrep.2016.10.006)
13. Fu F, Christakis NA, Fowler JH. 2017 Dueling biological and social contagions. *Sci. Rep.* **7**, 43634. (doi:10.1038/srep43634)
14. Bauch CT. 2005 Imitation dynamics predict vaccinating behaviour. *Proc. R. Soc. B* **272**, 1669–1675. (doi:10.1098/rspb.2005.3153)
15. Funk S, Gilad E, Watkins C, Jansen VA. 2009 The spread of awareness and its impact on epidemic outbreaks. *Proc. Natl Acad. Sci. USA* **106**, 6872–6877. (doi:10.1073/pnas.0810762106)
16. Betsch C, Böhm R, Korn L, Holtmann C. 2017 On the benefits of explaining herd immunity in vaccine advocacy. *Nat. Hum. Behav.* **1**, 0056. (doi:10.1038/s41562-017-0056)
17. Amin AB, Bednarczyk RA, Ray CE, Melchiori KJ, Graham J, Huntsinger JR, Omer SB. 2017 Association of moral values with vaccine hesitancy. *Nat. Hum. Behav.* **1**, 873–880. (doi:10.1038/s41562-017-0256-5)
18. Reluga TC, Bauch CT, Galvani AP. 2006 Evolving public perceptions and stability in vaccine uptake. *Math. Biosci.* **204**, 185–198. (doi:10.1016/j.mbs.2006.08.015)
19. Vardavas R, Breban R, Blower S. 2007 Can influenza epidemics be prevented by voluntary vaccination? *PLoS Comput. Biol.* **3**, e85. (doi:10.1371/journal.pcbi.0030085)
20. Fu F, Rosenbloom DI, Wang L, Nowak MA. 2011 Imitation dynamics of vaccination behaviour on social networks. *Proc. R. Soc. B* **278**, 42–49. (doi:10.1098/rspb.2010.1107)
21. Mbah MLN, Liu J, Bauch CT, Tekel YI, Medlock J, Meyers LA, Galvani AP. 2012 The impact of imitation on vaccination behavior in social contact networks. *PLoS Comput. Biol.* **8**, e1002469. (doi:10.1371/journal.pcbi.1002469)
22. Shim E, Chapman GB, Townsend JP, Galvani AP. 2012 The influence of altruism on influenza vaccination decisions. *J. R. Soc. Interface* **9**, 2234–2243. (doi:10.1098/rsif.2012.0115)
23. Wu ZX, Zhang HF. 2013 Peer pressure is a double-edged sword in vaccination dynamics. *EPL* (*Europhysics Letters*) **104**, 10002. (doi:10.1209/0295-5075/104/10002)
24. Oraby T, Thampi V, Bauch CT. 2014 The influence of social norms on the dynamics of vaccinating behaviour for paediatric infectious diseases. *Proc. R. Soc. B* **281**, 20133172. (doi:10.1098/rspb.2013.3172)
25. Bauch CT, Bhattacharyya S. 2012 Evolutionary game theory and social learning can determine how vaccine scares unfold. *PLoS Comput. Biol.* **8**, e1002452. (doi:10.1371/journal.pcbi.1002452)
26. Wang W, Liu QH, Cai SM, Tang M, Braunstein LA, Stanley HE. 2016 Suppressing disease spreading by using information diffusion on multiplex networks. *Sci. Rep.* **6**, 29259. (doi:10.1038/srep29259)
27. FINE PEM, Clarkson JA. 1986 Individual versus public priorities in the determination of optimal vaccination policies. *Am. J. Epidemiol.* **124**, 1012–1020. (doi:10.1093/oxfordjournals.aje.a114471)
28. Bauch CT, Galvani AP, Earn DJ. 2003 Group interest versus self-interest in smallpox vaccination policy. *Proc. Natl Acad. Sci. USA* **100**, 10 564–10 567. (doi:10.1073/pnas.1731324100)
29. Bauch CT, Earn DJ. 2004 Vaccination and the theory of games. *Proc. Natl Acad. Sci. USA* **101**, 13 391–13 394. (doi:10.1073/pnas.0403823101)
30. Galvani AP, Reluga TC, Chapman GB. 2007 Long-standing influenza vaccination policy is in accord with individual self-interest but not with the utilitarian optimum. *Proc. Natl Acad. Sci. USA* **104**, 5692–5697. (doi:10.1073/pnas.0606774104)
31. Hardin G. 2009 The tragedy of the commons? *J. Nat. Res. Policy Res.* **1**, 243–253. (doi:10.1080/19390450903037302)
32. Nyhan B, Reifler J, Richey S, Freed GL. 2014 Effective messages in vaccine promotion: a randomized trial. *Pediatrics* **133**, e835–e842. (doi:10.1542/peds.2013-2365)
33. Mclean AR, Blower SM. 1993 Imperfect vaccines and herd immunity to HIV. *Proc. R. Soc. Lond. B* **253**, 9–13. (doi:10.1098/rspb.1993.0075)
34. Mclean AR. 1995 Vaccination, evolution and changes in the efficacy of vaccines: a theoretical framework. *Proc. R. Soc. Lond. B* **261**, 389–393. (doi:10.1098/rspb.1995.0164)
35. Gandon S, Mackinnon MJ, Nee S, Read AF. 2001 Imperfect vaccines and the evolution of pathogen virulence. *Nature* **414**, 751–756. (doi:10.1038/414751a)
36. Anders JF, Jacobson RM, Poland GA, Jacobsen SJ, Wollan PC. 1996 Secondary failure rates of measles vaccines: a metaanalysis of published studies. *Pediatr. Infect. Dis. J.* **15**, 62–66. (doi:10.1097/00006454-199601000-00014)
37. Vandermeulen C, Roelants M, Vermoere M, Roseeuw K, Goubau P, Hoppenbrouwers K. 2004 Outbreak of mumps in a vaccinated child population: a question of vaccine failure? *Vaccine* **22**, 2713–2716. (doi:10.1016/j.vaccine.2004.02.001)
38. Lewnard JA, Grad YH. 2018 Vaccine waning and mumps re-emergence in the united states. *Sci. Transl. Med.* **10**, eaao5945. (doi:10.1126/scitranslmed.aao5945)
39. Baker JP. 2003 The pertussis vaccine controversy in Great Britain, 1974–1986. *Vaccine* **21**, 4003–4010. (doi:10.1016/S0264-410X(03)00302-5)
40. Burgess DC, Burgess MA, Leask J. 2006 The mmr vaccination and autism controversy in united kingdom 1998–2005: inevitable community outrage or a failure of risk communication? *Vaccine* **24**, 3921–3928. (doi:10.1016/j.vaccine.2006.02.033)
41. Larson HJ, Cooper LZ, Eskola J, Katz SL, Ratzan S. 2011 Addressing the vaccine confidence gap. *Lancet* **378**, 526–535. (doi:10.1016/S0140-6736(11)60678-8)
42. Brown KF, Long SJ, Ramsay M, Hudson MJ, Green J, Vincent CA, Kroll JS, Fraser G, Sevdalis N. 2012 Uk parents' decision-making about measles–mumps–rubella (mmr) vaccine 10 years after the mmr-autism controversy: a qualitative analysis. *Vaccine* **30**, 1855–1864. (doi:10.1016/j.vaccine.2011.12.127)
43. King C, Leask J. 2017 The impact of a vaccine scare on parental views, trust and information needs: a qualitative study in Sydney, Australia. *BMC Public Health* **17**, 106. (doi:10.1186/s12889-017-4032-2)
44. Larson HJ. 2018 Politics and public trust shape vaccine risk perceptions. *Nat. Hum. Behav.* **2**, 316. (doi:10.1038/s41562-018-0331-6)
45. Fine PE, Clarkson JA. 1987 Reflections on the efficacy of pertussis vaccines. *Rev. Infect. Dis.* **9**, 866–883. (doi:10.1093/clinids/9.5.866)
46. Nichol K, Margolis K, Wuorenma J, Von Sternberg T. 1994 The efficacy and cost effectiveness of vaccination against influenza among elderly persons living in the community. *New England J. Med.* **331**, 778–784. (doi:10.1056/NEJM199409223311206)
47. Edmunds W, Medley G, Nokes D. 1999 Evaluating the cost-effectiveness of vaccination programmes: a dynamic perspective. *Stat. Med.* **18**, 3263–3282. (doi:10.1002/(ISSN)1097-0258)
48. Basu S, Chapman GB, Galvani AP. 2008 Integrating epidemiology, psychology, and economics to achieve HPV vaccination targets. *Proc. Natl Acad. Sci. USA* **105**, 19 018–19 023. (doi:10.1073/pnas.0808114105)
49. van Boven M, Kretzschmar M, Wallinga JD, O'Neill P, Wichmann O, Hahné S. 2010 Estimation of measles vaccine efficacy and critical vaccination coverage in a highly vaccinated population. *J. R. Soc. Interface* **7**, 1537–1544. (doi:10.1098/rsif.2010.0086)
50. Beyer HL, Hampson K, Lembo T, Cleaveland S, Kaare M, Haydon DT. 2011 Metapopulation dynamics of rabies and the efficacy of vaccination. *Proc. R. Soc. B* **278**, 2182–2190. (doi:10.1098/rspb.2010.2312)
51. Medlock J, Pandey A, Parpia AS, Tang A, Skrip LA, Galvani AP. 2017 Effectiveness of unaids targets and hiv vaccination across 127 countries. *Proc. Natl Acad. Sci. USA* **114**, 4017–4022. (doi:10.1073/pnas.1620788114)
52. Sah P, Medlock J, Fitzpatrick MC, Singer BH, Galvani AP. 2018Optimizing the impact of low-efficacy influenza vaccines. *Proc. Natl Acad. Sci. USA* **115**, 5151–5156. (doi:10.1073/pnas.1802479115)
53. Horne Z, Powell D, Hummel JE, Holyoak KJ. 2015 Countering antivaccination attitudes. *Proc. Natl Acad. Sci. USA* **112**, 10 321–10 324. (doi:10.1073/pnas.1504019112)
54. Cappelen A, Mæstad O, Tungodden B. 2010 Demand for childhood vaccination: insights from behavioral economics. In *Forum for development studies*, vol. 37, pp. 349–364. London, UK: Taylor & Francis.

55. Miller E, Vurdien J, White J. 1992 The epidemiology of pertussis in England and Wales. *Commun. Dis. Rep. CDR Rev.* **2**, R152–R154.
56. Rohani P, Earn DJ, Grenfell BT. 2000 Impact of immunisation on pertussis transmission in england and wales. *Lancet* **355**, 285–286. (doi:10.1016/S0140-6736(99)04482-7)
57. Jansen VA, Stollenwerk N, Jensen HJ, Ramsay M, Edmunds W, Rhodes C. 2003 Measles outbreaks in a population with declining vaccine uptake. *Science* **301**, 804. (doi:10.1126/science.1086726)
58. Antona D, Lévy-Bruhl D, Baudon C, Freymuth F, Lamy M, Maine C, Floret D, Du Chatelet IP. 2013 Measles elimination efforts and 2008–2011 outbreak, France. *Emerg. Infect. Dis.* **19**, 357. (doi:10.3201/eid1903.121360)
59. Majumder MS, Cohn EL, Mekaru SR, Huston JE, Brownstein JS. 2015 Substandard vaccination compliance and the 2015 measles outbreak. *JAMA Pediatr.* **169**, 494–495. (doi:10.1001/jamapediatrics.2015.0384)
60. Maynard SJ. 1982 *Evolution and the theory of games*. Cambridge, UK: Cambridge University Press.
61. Nowak MA. 2006 *Evolutionary dynamics*. Cambridge, MA: Harvard University Press.
62. Hofbauer J, Sigmund K. 1998 *Evolutionary games and population dynamics*. Cambridge, UK: Cambridge University Press.
63. Rouderfer V, Becker NG, Hethcote HW. 1994 Waning immunity and its effects on vaccination schedules. *Math. Biosci.* **124**, 59–82. (doi:10.1016/0025-5564(94)90024-8)
64. Bauch CT, Sigdel R, Pharaon J, Anand M. 2016 Early warning signals of regime shifts in coupled human–environment systems. *Proc. Natl Acad. Sci. USA* **113**, 14 560–14 567. (doi:10.1073/pnas.1604978113)
65. Bertotti G. 1998 *Hysteresis in magnetism: for physicists, materials scientists, and engineers*. New York, NY: Academic Press.
66. Angeli D, Ferrell JE, Sontag ED. 2004 Detection of multistability, bifurcations, and hysteresis in a large class of biological positive-feedback systems. *Proc. Natl Acad. Sci. USA* **101**, 1822–1827. (doi:10.1073/pnas.0308265100)
67. Cross R. 1993 On the foundations of hysteresis in economic systems. *Econ. Phil.* **9**, 53–74. (doi:10.1017/S0266267100005113)
68. Treanor J. 2004 Influenza vaccine-outmaneuvering antigenic shift and drift. *New England J. Med.* **350**, 218–220. (doi:10.1056/NEJMp038238)
69. Pananos AD, Bury TM, Wang C, Schonfeld J, Mohanty SP, Nyhan B, Salathé M, Bauch CT. 2017 Critical dynamics in population vaccinating behavior. *Proc. Natl Acad. Sci. USA* **114**, 13 762–13 767. (doi:10.1073/pnas.1704093114)
70. Ibuka Y, Li M, Vietri J, Chapman GB, Galvani AP. 2014 Free-riding behavior in vaccination decisions: an experimental study. *PLoS ONE* **9**, e87164. (doi:10.1371/journal.pone.0087164)
71. Gillespie DT. 1977 Exact stochastic simulation of coupled chemical reactions. *J. Phys. Chem.* **81**, 2340–2361. (doi:10.1021/j100540a008)
72. Hauert C, Doebeli M. 2004 Spatial structure often inhibits the evolution of cooperation in the snowdrift game. *Nature* **428**, 643–646. (doi:10.1038/nature02360)
73. Traulsen A, Claussen JC, Hauert C. 2005 Coevolutionary dynamics: from finite to infinite populations. *Phys. Rev. Lett.* **95**, 238701. (doi:10.1103/PhysRevLett.95.238701)
74. Nowak MA, May RM. 1992 Evolutionary games and spatial chaos. *Nature* **359**, 826–829. (doi:10.1038/359826a0)
75. Durrett R, Levin S. 1994 The importance of being discrete (and spatial). *Theor. Popul. Biol.* **46**, 363–394. (doi:10.1006/tpbi.1994.1032)